



Published in final edited form as:

*J Leukoc Biol.* 2023 November 24; 114(6): 547–556. doi:10.1093/jleuko/qiad115.

## Deficiency of macrophage-derived Dnase1L3 causes lupus-like phenotypes in mice

Minal Engavale<sup>1</sup>, Colton J. Hernandez<sup>1,\*\*</sup>, Angelica Infante<sup>1</sup>, Tanya LeRoith<sup>2</sup>, Elliott Radovan<sup>1</sup>, Lauryn Evans<sup>1</sup>, Johanna Villarreal<sup>3</sup>, Christopher M. Reilly<sup>2</sup>, R. Bryan Sutton<sup>3</sup>, Peter A. Keyel<sup>1,\*</sup>

<sup>1</sup>Department of Biological Sciences, Texas Tech University, Lubbock, TX 79409, United States

<sup>2</sup>Department of Cell Biology and Physiology, Virginia Tech, Blacksburg, VA 24061, United States

<sup>3</sup>Department of Cell Physiology and Molecular Biophysics, Texas Tech University Health Sciences Center, Lubbock, TX 79430, United States

### Abstract

Systemic lupus erythematosus (SLE) is an autoimmune disease caused by environmental factors and loss of key proteins, including the endonuclease Dnase1L3. Dnase1L3 absence causes pediatric-onset lupus in humans, while reduced activity occurs in adult-onset SLE. The amount of Dnase1L3 that prevents lupus remains unknown. To genetically reduce Dnase1L3 levels, we developed a mouse model lacking *Dnase1L3* in macrophages (conditional knockout [cKO]). Serum Dnase1L3 levels were reduced 67%, though Dnase1 activity remained constant. Homogeneous and peripheral antinuclear antibodies were detected in the sera by immunofluorescence, consistent with anti-double-stranded DNA (anti-dsDNA) antibodies. Total immunoglobulin M, total immunoglobulin G, and anti-dsDNA antibody levels increased in cKO mice with age. The cKO mice developed anti-Dnase1L3 antibodies. In contrast to global Dnase1L3<sup>-/-</sup> mice, anti-dsDNA antibodies were not elevated early in life. The cKO mice had minimal kidney pathology. Therefore, we conclude that an intermediate reduction in serum Dnase1L3 causes mild lupus phenotypes, and macrophage-derived Dnase1L3 helps limit lupus.

\*Corresponding author: Department of Biological Sciences, Texas Tech University, Biology Rm 108, Box 43131, Lubbock, TX 79409-3131, United States. peter.keyel@ttu.edu.

\*\*Present address: Department of Pathology, University of Utah, Salt Lake City, UT 84112, United States

#### Author contributions

M.E.: Conceptualization, Investigation, Data curation—Formal analysis, Visualization, Validation, Writing—Original Draft, Writing—Review and Editing. C.J.H.: Investigation, Data curation—Formal analysis, Visualization, Writing—Original Draft, Writing—Review and Editing. A.I.: Investigation, Data curation—Formal analysis, Visualization, Writing—Original Draft, Writing—Review and Editing. T.L.: Investigation, Data curation—Formal analysis, Writing—Review and Editing. E.R.: Investigation, Data curation—Formal analysis, Writing—Original Draft, Writing—Review and Editing. L.E.: Investigation, Data curation—Formal analysis, Writing—Review and Editing. J.V.: Investigation, Resources, Writing—Review and Editing. C.M.R.: Validation, Data curation—Formal analysis, Writing—Review and Editing, Project Administration. R.B.S.: Validation, Resources, Writing—Review and Editing, Funding Acquisition, Project Administration. P.A.K.: Conceptualization, Investigation, Validation, Data curation—Formal analysis, Supervision, Writing—Original Draft, Writing—Review and Editing, Funding Acquisition, Project Administration.

#### Supplementary material

Supplementary materials are available at *Journal of Leukocyte Biology* online.

#### Conflicts of interest

P.A.K. and R.B.S. have patents pending on Dnase1L3 modifications to improve serum half-life.

## Keywords

apoptotic bodies; autoantibody; Dnase; dnase1L3; lupus; macrophage

---

## 1. Introduction

Systemic lupus erythematosus (SLE) is a challenging autoimmune disease to treat due to the disease heterogeneity. One key to unraveling the genetic heterogeneity of SLE are mutations in single genes that cause monogenic SLE. One gene associated with monogenic SLE in both humans and mice is the serum endonuclease *Dnase1L3*.<sup>1,2</sup> *Dnase1L3* loss in humans causes familial, pediatric-onset lupus with 100% penetrance, average onset by age 6 yr, no gender bias, high (~64%) incidence of lupus nephritis, and high antinuclear antibodies (ANAs) and anti-double-stranded DNA (anti-dsDNA) antibodies.<sup>1</sup> Partial loss of Dnase1L3 via activity-reducing mutations causes the related, lethal disease hypocomplementemic urticarial vasculitis syndrome.<sup>3-5</sup> Reduced Dnase1L3 serum activity occurs in human adult-onset SLE,<sup>2,6,7</sup> partly due to neutralizing autoantibodies targeting Dnase1L3.<sup>8,9</sup> Dnase1L3 is secreted primarily by macrophages and dendritic cells (DCs),<sup>2,10</sup> with IL-4 polarized macrophages secreting more Dnase1L3.<sup>11</sup> Dnase1L3 is upstream of T/B cell responses, inflammation, and complement. Thus, reduced Dnase1L3 activity contributes to SLE disease heterogeneity and to pathogenesis.

Understanding the pathogenesis caused by loss of Dnase1L3 activity is complicated by a second serum endonuclease, Dnase1. Both endonucleases belong to the Dnase1 family, and degrade cell-free DNA in the serum.<sup>12</sup> While Dnase1 was implicated in lupus-like phenotypes in mice,<sup>13</sup> recent work showed that B6 mice lacking Dnase1 do not develop lupus-like phenotypes, nor does loss of Dnase1 exacerbate lupus-like phenotypes in *Dnase1L3*<sup>-/-</sup> mice.<sup>14</sup> One key difference between Dnase1 and Dnase1L3 is a disordered C-terminus that enables digestion of DNA complexed with proteins and lipids.<sup>2,15,16</sup> Both nucleases can degrade plasmid DNA, termed Dnase1 family activity here. Dnase1L3 has a second, specific activity against complexed DNA that is essential for preventing SLE.

A mutant Dnase1L3 with reduced activity is expressed in both NZB/W F1 and MRL/lpr polygenic lupus mouse models.<sup>17</sup> Lupus-like phenotypes arise in strains not prone to autoimmunity (i.e. pure C57Bl/6 background) when *Dnase1L3* is globally eliminated.<sup>2,10</sup> Global *Dnase1L3*<sup>-/-</sup> mice produce anti-dsDNA antibodies starting in the first 2 months of life, and expand B cells and neutrophils expand in the first 8 to 14 wk.<sup>2,10,14</sup> However, the full repertoire of autoantibodies does not develop until ~50 wk.<sup>2</sup> By 50 wk of age, *Dnase1L3*<sup>-/-</sup> mice develop splenomegaly with spontaneous germinal center formation, glomerulonephritis, and kidney immunoglobulin G (IgG) deposition.<sup>2,18</sup> Pathological changes in the kidney are considered mild.<sup>2</sup> Thus, mice can model pathogenesis in the absence of Dnase1L3 and its impact on specific lupus phenotypes.

One unknown remaining is the amount of Dnase1L3 needed to prevent disease. Because partial reduction of Dnase1L3 activity contributes to sporadic lupus<sup>3,8</sup> and hypocomplementemic urticarial vasculitis syndrome, we aimed to determine how partial reduction of Dnase1L3 impacts autoimmunity in B6 mice. To test how partial reduction of

Dnase1L3 impacts lupus-like phenotypes, we generated a Dnase1L3 cell-specific knockout mouse model. In this model, loss of *Dnase1L3* from macrophages caused mild lupus-like phenotypes. Autoantibodies were generated, including anti-dsDNA antibodies, though onset was delayed compared with global *Dnase1L3*<sup>-/-</sup>. Kidney damage in these mice was mild. These data reveal the lupus-like phenotypes most affected by partial Dnase1L3 loss, and suggest maintaining healthy serum Dnase1L3 activity is crucial to preventing autoimmunity.

## 2. Methods

### Reagents

All reagents were from Thermo Fisher Scientific unless otherwise specified. Gel red was from Biotium. Taq DNA polymerase was from Syd Labs. The anti-human Dnase1L3 rabbit polyclonal antibodies were obtained from Abnova (Cat#H00001776-W01P) and Genetex (Cat#GTX114363). The anti-dsDNA monoclonal antibody clone autoanti-dsDNA was deposited to the Developmental Studies Hybridoma Bank by E.W. Voss. It was obtained from the Developmental Studies Hybridoma Bank created by the National Institute of Child Health and Human Development of the National Institutes of Health and maintained at the University of Iowa, Department of Biology (Iowa City, IA, USA). Rat anti-mouse complement protein 3 (C3) was from NOVUS Biologicals (Cat#NB200-540). Mouse IgG (Cat#015-000-002), anti-mouse IgG (Cat#115-005-003), and anti-mouse IgM (Cat#715-005-020) antibodies were obtained from Jackson ImmunoResearch. Mouse IgM (Cat#MGM00) was from Invitrogen. horseradish peroxidase (HRP)-conjugated anti-mouse IgG (Cat#115-035-146), HRP-conjugated anti-mouse IgM (Cat#115-035-075), and Cy3-conjugated anti-mouse IgM (Cat#115-165-075) were from Jackson ImmunoResearch. Anti-rat IgG conjugated to Alexa Fluor 647 and anti-mouse IgG conjugated to Alexa Fluor 488 were from Invitrogen. Commercial HEp-2 cells and ANA staining reagents were from MBL Bion. GFP-Lamp1 cloned in pCS2 + was used for Dnase1 assays, as previously described.<sup>15</sup> Mouse Dnase1L3 lacking the signal sequence was cloned into p202 using BamHI and XhoI restriction sites. Recombinant human Dnase1L3 in p202 was previously described.<sup>15</sup> Recombinant proteins were purified as previously described.<sup>15</sup>

### Animals

B6.129P2-Lyz2<sup>tm1(cre)Ifo</sup>/J (LysM-Cre) mice (Strain #004781) were obtained from the Jackson Laboratory and housed at Texas Tech University under the oversight of the Texas Tech University Institutional Animal Care and Use Committee. C57BL/6Ncr1-Dnase113<sup>em1(IMPC)Mbp/Mmucd</sup> (Dnase1L3<sup>-/-</sup>) (MMRRC: 067429-UCD) were obtained from the Mutant Mouse Resource and Research Centers at the University of California, Davis. Dnase1L3<sup>fl/fl</sup> mice were generated by inGenious Targeting Laboratory. A loxP site was introduced upstream of exon 3, which encodes the active site of the Dnase1L3 gene, while a neomycin resistance cassette flanked by FRT sites and a second loxP site was inserted downstream of exon 4 (Supplementary Fig. S1). After removal of the neomycin cassette by breeding to FLP deleter mice, heterozygotes were crossed to generate mice with 2 floxed alleles (Dnase1L3<sup>fl/fl</sup>). The breeding scheme to generate macrophage-specific Dnase1L3 knockouts involved crossing the Dnase1L3<sup>fl/fl</sup> mice with LysM-Cre transgenic mice that express Cre recombinase specifically in myeloid cells including macrophages.

This caused deletion of Dnase1L3 in macrophages in the offspring. Mice were born with the expected Mendelian ratio, 25% Dnase1L3<sup>fl/fl</sup>×LysM-Cre<sup>+/-</sup> (conditional knockout [cKO]), 25% Dnase1L3<sup>fl/+</sup>×LysM-Cre<sup>+/-</sup> (heterozygous), and 50% Dnase1L3<sup>fl/fl</sup>×LysM-Cre<sup>-/-</sup> (wild-type [WT]). The cKO mice were genotyped by polymerase chain reaction (PCR) using primers specific to the Cre and Dnase1L3. The sample size for each experiment was determined based on a power analysis using estimated effect sizes. No randomization was necessary, so this method was not employed in the study. For blinding, mice were numbered and the experimentalist was blinded to the mouse genotype during the assay. Kidney pathology was read in a blinded fashion by a board-certified pathologist (T.L.).

## Genotyping

Genomic DNA from tissue biopsies (tail snips or ear punches) was isolated using a Chelex method,<sup>19</sup> or an optimized Proteinase K method.<sup>20</sup> For the Chelex method, tissue samples were ground into a uniform suspension in nuclease-free water and mixed with autoclaved 1% saponin (Sigma-Aldrich) in 1 × phosphate-buffered saline (PBS). After a 20 min room temperature incubation, samples were centrifuged at 17,000 *g* for 2 min. The pellet was washed once in 1 × PBS and vortexed in sterile nuclease-free water. Chelex 100 sodium resin (Bio-Rad) was added to 4% (w/v) final concentration. Samples were heated at 95 °C for 12 min and then centrifuged at 17,000 *g* for 2 min. The supernatant containing genomic DNA was used for downstream analysis. For the optimized Proteinase K method, tissue samples were incubated overnight in lysis buffer containing Proteinase K (100 mM Tris, 5 mM EDTA, 0.2% SDS, 200 mM NaCl, 0.4 mg/mL Proteinase K [Sigma-Aldrich], pH 8.5) at 55 °C. The next day, ethanol was added to 70% final volume and samples centrifuged at 16,000 *g* for 30 min. The pellet was washed 3 times with 70% ethanol and centrifuged at 16,000 *g* for 20 min each time. After the final wash, the genomic DNA was resuspended in 1 × TE buffer (100 mM Tris, pH 5.0, 1 mM EDTA, 10 mM NaCl) and stored at -20 °C.

PCR genotyping was performed using primers from IDT. Primers used for Dnase1L3<sup>fl/fl</sup> mice were WT1 (5'-GGG CTG GCA TAG AGC ATC AT-3') and SC1 (5'-CAA CTT GAT GTG AAA GGT GGT AGT G-3'). Primers used for LysM-Cre were oIMR3066 (5'-CCC AGA AAT GCC AGA TTA CG-3'), oIMR3067 (5'-CTT GGG CTG CCA GAA TTT CTC-3'), and oIMR3068 (5'-TTA CAG TCG GCC AGG CTG AC-3'). PCR was performed using the following algorithm: an initial denaturation step at 94 °C for 5 min, followed by 34 cycles of denaturation at 94 °C for 30 s, annealing at 56 °C for 30 s, and extension at 72 °C for 30 s, followed by a final extension step at 72 °C for 5 min. PCR products were analyzed on a 2% agarose gel. The LysM-Cre band was 700 bp, with 350 bp band for WT. The floxed Dnase1L3 allele was detected at 525 bp, while the wild type allele was detected at 476 bp.

## Dnase1L3 antibody

Mouse Dnase1L3 was purified as previously described<sup>15</sup> and concentrated to 5 mg/mL at 95% purity. Two New Zealand White rabbits were immunized and bled by Pacific Immunology, as overseen by their Institutional Animal Care and Use Committee. After bleeding to collect preimmune serum, rabbits were immunized once in complete Freund's adjuvant, a second time on day 21 in incomplete Freund's adjuvant, a third time on day 42 in

incomplete Freund's adjuvant, and a fourth time on day 70 in incomplete Freund's adjuvant. Antisera were collected on days 49, 63, 77, and 91, with final exsanguination bleeds on days 98 and 101. Antibody validation is summarized in Supplementary Fig. S2.

### Enzyme-linked immunosorbent assay

Total IgG and IgM levels from mouse sera were determined as described.<sup>21</sup> A 96-well enzyme-linked immunosorbent assay (ELISA) plate was coated with goat anti-mouse IgG or goat anti-mouse IgM capture antibody overnight at 4 °C. Wells were washed 3 times in 1 × PBS with 0.05% Tween 20 (PBST), and blocked with 1% bovine serum albumin (BSA) in PBST for 2 h at room temperature. Mouse IgG or mouse IgM was used as standards, while mouse sera samples were diluted 1:5,000 in 1% BSA in PBST. After 2 h, plates were washed 3 × in PBST, incubated with HRP-conjugated goat anti-mouse IgG or IgM antibody at 1:20,000 and 1:10,000 respectively, and developed using 0.2 mg/mL TMB (Sigma-Aldrich), 0.015% H<sub>2</sub>O<sub>2</sub> in 100 mM sodium acetate, pH 5.5. The reaction was stopped with 0.5 M H<sub>2</sub>SO<sub>4</sub>. A<sub>450</sub> was measured on a Powerwave Microplate Spectrophotometer running Gen5 Data Analysis Software (BioTek) and antibody concentration determined.

Anti-dsDNA antibodies were measured as described.<sup>21</sup> The 96 well ELISA plates were precoated with 0.05 mg/mL poly-L-lysine at room temperature for 20 min, washed with 1 × nuclease-free water, and coated with 5 µg/mL calf thymus DNA (Sigma-Aldrich) overnight at 4 °C. After washing 3 × in PBST, plates were blocked for 1 h at room temperature with 1% BSA in PBST. Anti-dsDNA (clone autoanti-dsDNA) antibody was used as a standard, starting at 500 pg/mL. Mouse sera were diluted 1:500 in 1% BSA in PBST at RT for 2 h. After 2 h, plates were washed 3 × in PBST, incubated with HRP-conjugated goat anti-mouse IgG antibody at 1:10,000, and developed using 0.2 mg/mL TMB, 0.015% H<sub>2</sub>O<sub>2</sub> in 100 mM sodium acetate, pH 5.5. The reaction was stopped with 0.5 M H<sub>2</sub>SO<sub>4</sub>. A<sub>450</sub> was measured and antibody concentration determined.

Anti-histone and anti-Smith (anti-Sm) antibodies were measured using commercially available kits according to the manufacturer's instruction (Alpha Diagnostics).

To measure the Dnase1L3 levels from mouse serum, 96-well plates were coated with 1:500 of serum diluted in 1 × PBS, or with a standard curve starting at 25 ng/mL of recombinant mouse Dnase1L3, overnight at 4 °C. After overnight incubation and washing 3 × in PBST, plates were blocked for 1 h at room temperature with 1% BSA in PBST. Then anti-mouse Dnase1L3 immune serum was added at 1:5,000 for 2 h at room temperature. Plates were washed 3 × in PBST, incubated with HRP-conjugated goat anti-rabbit IgG antibody (1:10,000), and developed using 0.2 mg/mL TMB, 0.015% H<sub>2</sub>O<sub>2</sub> (Walmart) in 100 mM sodium acetate, pH 5.5. The reaction was stopped with 0.5 M H<sub>2</sub>SO<sub>4</sub>. A<sub>450</sub> was measured and the Dnase1L3 concentration determined.

To measure the anti-Dnase1L3 antibody titer, 96-well ELISA plates were coated with 5 µg/mL recombinant murine Dnase1L3 overnight at 4 °C. Plates were then washed 3 × in PBST, and blocked for 1 h at room temperature using 1% BSA in PBST. Mouse serum was added at 1:50 for 2 h at 37 °C. Plates were washed 3 × in PBST, incubated with HRP-conjugated goat anti-mouse IgG antibody (1:10,000), and developed using 0.2 mg/mL

TMB, 0.015% H<sub>2</sub>O<sub>2</sub> in 100 mM sodium acetate, pH 5.5. The reaction was stopped with 0.5 M H<sub>2</sub>SO<sub>4</sub>. A<sub>450</sub> was measured and the anti-Dnase1L3 titer was determined to be positive if the A<sub>450</sub> was greater than 0.1.

### Serum DNA assay

To measure DNA from the mouse serum, DNA was first isolated from the serum using the E.Z.N.A. DNA extraction kit. This DNA was quantified using the QuantiFluor dsDNA System (Promega). A standard curve was generated by linear regression of 2-fold serial plasmid DNA dilutions starting from 100 ng/mL.

### Dnase1 assay

Dnase1 family assays were performed as described.<sup>15,22</sup> Briefly, 200 ng of plasmid DNA was incubated with varying concentrations of mice sera alone in Dnase assay buffer (20 mM Tris, pH 7.4, 5 mM MgCl<sub>2</sub>, 2 mM CaCl<sub>2</sub>) for 30 min at 37 °C. The extent of DNA degradation was quantitated by measuring the integrated intensity of degraded and intact plasmid DNA from gel red-stained agarose gels using Photoshop Creative Suite (Adobe) and determining the percent degradation. The EC<sub>50</sub> for plasmid degradation was calculated from the dose-response curve using regression on the linear portion of the curve.

### Immune Complex Assay

Immune complex degradation was assayed as described.<sup>15</sup> ELISA plates were precoated with 0.05 mg/mL poly-L-lysine at room temperature for 20 min, washed with 1 × nuclease-free water, and coated with 5 µg/mL calf thymus DNA overnight at 4 °C. After washing 3 × in PBST and blocking for 1 h at room temperature using 1% BSA in PBST, 250 pg/mL anti-dsDNA antibody was added to all wells except the standard curve. The standard curve received 2-fold dilutions of anti-dsDNA antibody starting at 500 pg/mL. After 1 h, the plates were washed 3 × in PBST, then mouse serum or recombinant Dnase1L3 (diluted into Dnase assay buffer) was added, and plates incubated at 37 °C for 2 h. Plates were washed 3 × in PBST, incubated with HRP conjugated goat anti-mouse IgG antibody (1:20,000), and developed using 0.2 mg/mL TMB, 0.015% H<sub>2</sub>O<sub>2</sub> in 100 mM sodium acetate, pH 5.5. The reaction was stopped with 0.5 M H<sub>2</sub>SO<sub>4</sub>. The A<sub>450</sub> was measured and antibody concentration in each well calculated. The amount of anti-dsDNA antibody remaining in the well was measured by linear regression from the standard curve.

Three variations to this assay were used. To deplete any murine antibodies potentially interfering with the assay, protein G beads were incubated with 2 µl mouse serum at 4 °C for 30 min. The serum and beads were centrifuged at 10,000 *g* for 10 min at 4 °C to pellet the beads. Then, the serum was used in the assay. In a second variation, a 50% matrix diluent (Surmodics) and 50% Dnase assay buffer was used to dilute the serum instead of 1 × Dnase assay buffer. Finally, the method of standard additions was used. A known amount of murine Dnase1L3 was added to each dilution of mouse serum to a final concentration of 0.125 µg/mL to ensure activity would fall along the standard curve.

## Histopathology

Kidneys were fixed with 4% paraformaldehyde, dehydrated in 30% sucrose, and embedded in Tissue-Plus O.C.T. Compound (Scigen), and flash frozen in isopentane followed by liquid nitrogen. Tissues were cut into 5- $\mu$ m cryosections using a Leica CM1950. Sections were stained with hematoxylin and eosin. Kidney inflammation was evaluated as previously described.<sup>23</sup> Hypercellularity, mesangial proliferation, necrosis, sclerosis, and tubulointerstitial and perivascular inflammation were scored separately on a scale ranging from 0 (none) to 4 (highest), and the cumulative score was calculated. Images were captured using an Olympus BX41 microscope equipped with a 60  $\times$  (1.40 NA) objective running QCapture Pro 7 (QImaging) and processed by ImageJ software version 1.54f (National Institutes of Health).

## Immunofluorescence

Immunofluorescence was performed on 5- $\mu$ m kidney cryosections. The sections were fixed for 15 min in 2% paraformaldehyde, permeabilized and blocked for 15 min in 10% goat serum and 0.05% saponin. The sections were then stained with rat anti-mouse C3 monoclonal antibody for 1 h, followed by goat anti-mouse IgG conjugated to Alexa Fluor 488, goat anti-mouse IgM conjugated to Cy3, and goat anti-rat IgG conjugated to Alexa Fluor 647 for 1 h, and finally DAPI stained. The sections were imaged using a Fluoview 3000 confocal microscope (Olympus) equipped with a 60  $\times$ , 1.42 NA oil immersion objective. The deposition of IgG, IgM immune complexes, and C3 was determined by measuring the integrated intensities using ImageJ software. The images were analyzed by splitting each image into RGB channels. All fluorescence-integrated density values were normalized based on the area and respective backgrounds. Mean density values of each image were calculated, and data were recorded and graphed using GraphPad Prism 8.1 (GraphPad Software). The brightness and contrast of all confocal images were adjusted equally for qualitative purposes.

## ANA staining

ANAs were detected using fixed HEp-2 cells (MBL Bion) as a substrate. Mouse serum was incubated with HEp-2 cells at different dilutions (1:40, 1:160, 1:640), the slides were washed, and then the slides were stained with a goat anti-mouse IgG conjugated to Alexa Fluor 488, followed by staining in DAPI. The stained cells were imaged using a Fluoview 3000 confocal microscope equipped with a 60  $\times$ , 1.42 NA oil immersion objective. The images were processed using ImageJ. For qualitative purposes, the brightness and contrast were adjusted equally for all confocal images. At least 30 cells were evaluated per sample. Fields of cells with fluorescence  $>2$  SD over the negative control were considered positive.

## Sodium dodecyl sulfate–polyacrylamide gel electrophoresis and immunoblotting

Sodium dodecyl sulfate–polyacrylamide gel electrophoresis and immunoblotting were performed as described.<sup>24</sup> Briefly, samples were resolved on 10% polyacrylamide gels at 160 V for ~60 min and transferred to nitrocellulose in an ice bath with transfer buffer (15.6 mM Tris and 120 mM glycine) at 300 mA for 90 min. The blots were blocked using 5% skim milk in 10 mM Tris-HCl, pH 7.5, 150 mM NaCl, and 0.1% Tween 20. Portions of the

blot were incubated with 1 of the following primary antibodies for 2 h at room temperature or overnight: anti-human Dnase1L3 (1:1000) (Abnova and Genetex), preimmune rabbit serum (1:5000), or rabbit anti-mouse Dnase1L3 immune serum. Next, the blots were washed 3 × in TBST, incubated with HRP-conjugated anti-rabbit IgG antibodies (1:10,000), washed 3 × in TBST, and developed with enhanced chemiluminescence: 0.01% H<sub>2</sub>O<sub>2</sub>, 0.2 mM p-Coumaric acid (Sigma-Aldrich), 1.25 mM luminol (Sigma-Aldrich) in 0.1 M Tris (pH 8.4).

## Statistics

Prism 8.1 or Excel were used for statistical analysis. Data are represented as mean ± SEM as indicated. The EC<sub>50</sub> for Dnase1 family activity was calculated in Excel as previously described.<sup>25</sup> Exclusion criteria for data was failure of positive or negative controls. Statistical significance for normally distributed data was determined by 1- or 2-way analysis of variance with Tukey posttesting as specified;  $P < 0.05$  was considered to be statistically significant. Graphs were generated in Excel, Prism, and Photoshop (Adobe).

## 3. Results

### 3.1 Macrophages supply most serum Dnase1L3

To develop a mouse model with partially reduced Dnase1L3, we eliminated Dnase1L3 from macrophages. Macrophages were chosen instead of DCs because Dnase1L3 secretion and activity is better characterized in macrophages.<sup>11,17,22</sup> To generate cell specific Dnase1L3 cKO mice, loxP sites were introduced flanking exons 3 and exon 4 in B6 embryonic stem cells (Supplementary Fig. S1A). Mice homozygous for loxP sites flanking Dnase1L3 (Dnase1L3<sup>fl/fl</sup>) were crossed twice to LysM-Cre transgenic mice. Genotyping was confirmed by PCR (Supplementary Fig. S1B). We note that neutrophils and some DC subsets also express LysM, Dnase1L3 expression is expected to be decreased in them. Overall, we generated mice lacking *Dnase1L3* in macrophages.

We assessed these mice for Dnase1L3 levels and Dnase1 family activity. Serum was collected weekly from WT and cKO mice. To measure mouse Dnase1L3 from mouse serum, we generated polyclonal antibodies to murine Dnase1L3. Immune serum recognized both murine and human Dnase1L3 by Western blot and ELISA (Supplementary Fig. S2). By ELISA, serum Dnase1L3 levels were 67% reduced in cKO sera compared with WT (Fig. 1A). These results are consistent with previous results<sup>2</sup> using chlodronate liposomes to transiently deplete macrophages. Thus, depletion of Dnase1L3 from macrophages reduces serum Dnase1L3 levels.

We next measured serum Dnase1 family activity, which is the ability of nucleases to degrade naked DNA at neutral pH. Dnase1 family activity was measured by plasmid degradation, which both Dnase1 and Dnase1L3 can do.<sup>2,15,16</sup> We observed no difference in Dnase1 family activity between WT and cKO mouse sera (Fig. 1B). We failed to measure Dnase1L3-specific activity with either our immune complex degradation assay or barrier to transfection assay<sup>15</sup> because confounders in the serum interfered with these assays



(Supplementary Fig. S3). Overall, these data indicate that total serum Dnase1 family activity was not altered by partial Dnase1L3 loss.

### 3.2 Loss of Dnase1L3 from macrophages elevates total IgG and IgM antibody levels

We next compared serologic lupus-like phenotypes between WT and cKO mice. To monitor disease progression, we collected serum weekly over each mouse's lifespan. To measure overall autoantibody induction, we measured total IgG and IgM levels. Neither antibody subtype was elevated in the first 30 wk. At 31 to 40 wk, total IgM levels increased (Fig. 2A-B), but total IgG did not (Fig. 2C-D). By 41 to 50 wk of age, both total IgG and IgM levels were elevated 2-fold in cKO mice compared with WT mice (Fig. 2). Comparing antibody levels over time revealed a steady increase in both IgM and IgG (Fig. 2B, D) for cKO mice. We did not observe any sex-specific differences in elevation of total IgM or total IgG (Fig. 2). These data suggest that reduced levels of Dnase1L3 cause late elevation of autoantibodies.

### 3.3 Partial loss of Dnase1L3 delays onset of anti-dsDNA antibodies

Because total antibody levels were increased in cKO mice, we tested autoantibody production. We found that neither anti-Smith nor anti-histone antibodies were produced by cKO mice (Supplementary Fig. S4A-C). We measured ANA titers using commercial Hep-2 cell preparations. In contrast to WT mice, cKO mice had positive ANA titers at the highest dilution tested, 1:640 (Fig. 3A-B). In cKO mice, the ANA staining pattern was homogeneous and perinuclear (Fig. 3A). These staining patterns are characteristic of SLE, typically associated with anti-DNA autoantibodies. We compared anti-DNA antibodies between WT and cKO mice. Anti-dsDNA antibodies were elevated at 31 to 40 wk (Fig. 3C). Female mice showed a greater difference in anti-dsDNA levels compared with male mice (Fig. 3C). When examined longitudinally, both sexes showed significant increases in anti-dsDNA antibody levels with age (Fig. 3D). These results contrast with a prior analysis of global Dnase1L3<sup>-/-</sup> mice,<sup>2</sup> which had elevated anti-dsDNA antibodies starting at 4 wk of age. We compared cKO mice to a different global Dnase1L3<sup>-/-</sup> mouse (FKO) and to MRL/lpr. The MRL/lpr mouse had 4 to 5 × anti-dsDNA antibodies compared with cKO, while FKO had slightly more (Supplementary Fig. S4D). Overall, partial loss of Dnase1L3 was sufficient to generate anti-dsDNA antibodies.

We next explored the mechanism of anti-dsDNA antibody elevation in these mice. We measured serum cell-free DNA levels, to determine if partial loss of Dnase1L3 elevated circulating DNA. While we observed a significant difference in DNA levels between wild type and FKO mice, cKO appeared intermediate (Fig. 3E). We next used recombinant mouse Dnase1L3 to measure anti-Dnase1L3 antibodies in WT or cKO mice. In contrast to WT mice, where 2 of 6 mice had anti-Dnase1L3 antibodies, all cKO mice had elevated anti-Dnase1L3 antibodies (Fig. 3F). These data suggest partial loss of Dnase1L3 enables the generation of anti-Dnase1L3 antibodies, which could account for the pathology observed when Dnase1L3 is reduced.

### 3.4 Dnase1L3 cKO mice have mild kidney phenotypes

We compared kidney pathology between cKO and WT littermate control mice. We euthanized the mice at 50 wk of age and analyzed their kidneys. Glomeruli had an increased diameter, due to increased thickness of the Bowman's space in both male and female mice (Fig. 4A-C). Kidney pathology scores were elevated, especially in female cKO mice (Fig. 4D). Phenotypes associated with lupus nephritis, including mesangiopathy, hypercellularity, and segmental glomerulonephritis were observed in a subset of the cKO mice, with a greater proportion of female cKO mice showing phenotypes compared with male cKO mice (Fig. 4D). However, the overall score based on these phenotypes was lower than usually observed in polygenic lupus models. This suggests that partial Dnase1L3 loss does not drive robust kidney pathology.

We measured immune complex deposition in the kidneys by immunofluorescence. IgG, IgM, and C3 deposited in the glomeruli of cKO but not in the WT mice (Fig. 4E). We observed fine granular immune complexes and complement deposition in and around the glomeruli (Fig. 4E). We quantitated immune complex deposition in the glomeruli. IgG, IgM, and C3 were elevated in cKO mice (Fig. 4F). These data suggest that partial loss of Dnase1L3 contributes to mild kidney lupus-like phenotypes.

Finally, we compared the lupus-like phenotypes we measured across mice to determine any trends in these phenotypes. We scaled each phenotype to a 5 point scale, with 5 representing the maximal phenotype and 0 representing the minimum phenotype. Using this scale, we observed an inverse relationship between Dnase1L3 levels and the serology and kidney phenotypes (Fig. 5). Due to the mildness of the kidney phenotypes, smaller differences were observed between cKO and WT mice. Overall, we conclude that partial Dnase1L3 loss triggers mild lupus-like phenotypes in mice.

## 4. Discussion

In this study, we developed a genetic model of partial Dnase1L3 deficiency by eliminating *Dnase1L3* from macrophages. We used these mice to evaluate the impact of partial Dnase1L3 deficiency on the development of lupus-like phenotypes in mice. While deletion of *Dnase1L3* from macrophages reduced serum Dnase1L3, it did not reduce Dnase1 family activity. We found that partial loss of Dnase1L3 increased total IgM, total IgG and autoantibody levels. It caused a delayed increase in anti-dsDNA antibody production relative to full Dnase1L3<sup>-/-</sup> mice. We detected anti-Dnase1L3 antibodies in these mice. In contrast, kidney damage was minimal. These results suggest that a partial loss of Dnase1L3 is sufficient to initiate lupus-like phenotypes in mice. Thus, restoring Dnase1L3 may be one promising approach to treat SLE.

While LysM-specific depletion of Dnase1L3 reduced serum Dnase1L3 67%, it did not alter serum Dnase1 family activity. Serum Dnase1 family activity is provided by Dnase1 and Dnase1L3. This lack of impact on activity could be due to a lower abundance of serum Dnase1L3. In our system, Dnase1L3 production by unaffected cell types failed to compensate for reduced myeloid expression. Alternatively, compensatory Dnase1 expression could correct reduced Dnase1L3 activity at the level of bulk DNA degradation. Dnase1

may compensate for Dnase1L3 activity under certain circumstances.<sup>26</sup> Polygenic lupus mouse models attempt to compensate for decreased Dnase1L3 activity by elevating Dnase1L3 expression.<sup>17</sup> While Dnase1 can compensate for Dnase1 family activity, Dnase1 cannot rescue many Dnase1L3-specific activities, like generating extracellular circular chromosomal DNA,<sup>27</sup> clearing multinucleosome cell-free DNA,<sup>28,29</sup> and preventing lupus onset.<sup>2,14</sup> Overall, this suggests that compensatory feedback mechanisms are inadequate to prevent onset of autoimmunity.

Our work provides new insight into lupus heterogeneity and disease onset. Global Dnase1L3<sup>-/-</sup> mice produce anti-dsDNA antibodies early in life.<sup>2,10,14</sup> In contrast, partial loss of Dnase1L3 delayed onset of anti-dsDNA antibodies until 40 to 50 wk. Interestingly, anti-dsDNA IgG was elevated along with IgM levels, prior to the global increase in IgG. This suggests a gradual accumulation of antigenic extracellular DNA underlies the trigger for lupus-like phenotypes. The delayed onset of autoantibodies in our model of partial Dnase1L3 loss is similar to human lupus, where onset often occurs in early adulthood.<sup>30</sup> Importantly, neutralization of Dnase1L3 by autoantibodies occurs in ~50% of sporadic lupus.<sup>8</sup> Similar to humans, our mice developed anti-Dnase1L3 antibodies when Dnase1L3 was partially reduced. The potential for cross-reactivity between anti-DNA and anti-Dnase1L3<sup>9</sup> autoantibodies suggests a negative feedback loop that accelerates disease. Future work is needed to determine if these antibodies are anti-DNA antibodies that also target Dnase1L3, if they are anti-Dnase1L3 antibodies that also target DNA, or if a DNA/Dnase1L3 complex generates antibodies simultaneously.

There are several mechanisms by which partial Dnase1L3 loss could drive disease. One mechanism is accumulation of cell-free DNA. While we did not observe a statistically significant elevation in total cell-free DNA, the cell-free DNA profile is altered when Dnase1L3 is absent.<sup>28</sup> This DNA could be more antigenic, driving anti-DNA antibodies that cross-react with Dnase1L3, creating the negative feedback loop. Alternatively, when Dnase1L3 is reduced, the amount of antigenic, complexed DNA could increase, causing an increase in microparticles. However, we were unable to measure microparticles. Our myeloid-specific Dnase1L3 knockout represents a genetic system to further explore how partial loss of Dnase1L3 affects the development of autoantibodies.

Along with insight into autoantibody onset, we provide evidence on organ-system specific lupus defects. Kidney phenotypes from mice with loss of macrophage Dnase1L3 were mild. Kidney pathologies more typically associated with lupus were mild and present only in a subset of mice. This mild kidney phenotype suggests that loss of macrophage-derived Dnase1L3 is not a major driver of kidney pathology. While the late onset of autoantibodies may have delayed the kidney pathology, similar results from the global knockouts<sup>2</sup> suggest that Dnase1L3 is not uniquely necessary to prevent lupus nephritis in mice. Dnase1 might rescue kidney phenotypes. For example, Dnase1 rescues renal pathology in *Staphylococcus aureus* infection of Dnase1<sup>-/-</sup>/Dnase1L3<sup>-/-</sup> mice.<sup>14</sup> Overall, these results provide new insight into our understanding of lupus disease heterogeneity.

Our work opens new avenues of research in the field of lupus and nucleases. One avenue is determining if the impact of DC-specific deficiency of Dnase1L3 phenocopies our mice.

Our findings suggest that restoration of Dnase1L3 is a viable therapeutic strategy for SLE. Further research is needed to establish the therapeutic potential of Dnase1L3 in SLE.

While we generated and characterized a mouse model with partial Dnase1L3 loss, our work had limitations. Our assessment of lupus-like phenotypes was restricted to serology and kidney pathology. We did not evaluate T cell or B cell subsets nor behavior. Besides anti-dsDNA autoantibodies, we characterized limited autoantibody subsets. While Dnase1L3 is elevated in M2a macrophages,<sup>11</sup> we did not measure macrophage polarization in Dnase1L3 deficient macrophages in vivo. Finally, we did not test the intracellular roles for Dnase1L3.<sup>22,27</sup>

Overall, our study highlights the importance of optimal levels of Dnase1L3 in preventing SLE. Our Dnase1L3 cKO mouse provides a model where partial loss of Dnase1L3 can be modeled. This model expands the repertoire and physiology of lupus mouse models, providing insights into the impact of variable levels of Dnase1L3 on lupus-like disease heterogeneity in mice.

## Supplementary Material

Refer to Web version on PubMed Central for supplementary material.

## Acknowledgments

The authors thank members of the Keyel lab for critical review of the manuscript. They thank the College of Arts & Sciences Microscopy for use of facilities.

## Funding

This work was supported by Texas Tech University (P.A.K.), American Heart Association grant 16SDG30200001 (P.A.K.), and Lupus Research Alliance grant 707050 (P.A.K.). C.J.H. was supported by the Texas Tech University, Ronald E. McNair Post-Baccalaureate Achievement Program, U.S. Department of Education Grant, 2017–2022. A.I. was supported by the Plains Bridges to the Baccalaureate National Institutes of Health grant R25GM083730. The funders had no role in the design of the study; in the collection, analysis, or interpretation of data; in the writing of the manuscript; nor in the decision to publish the results. The content is solely the responsibility of the authors and does not necessarily represent the official views of the funding agencies.

## Data availability

All data are available in the main text or the Supplementary materials.

## References

1. Al-Mayouf SM, Sunker A, Abdwani R, Arawi SA, Almurshedi F, Alhashmi N, Al Sonbul A, Sewairi W, Qari A, Abdallah E, et al. Loss-of-function variant in DNASE1L3 causes a familial form of systemic lupus erythematosus. *Nat Genet.* 2011;43(12):1186–1188. 10.1038/ng.975 [PubMed: 22019780]
2. Sisirak V, Sally B, D'Agati V, Martinez-Ortiz W, Ozcakar ZB, David J, Rashidfarrokhi A, Yeste A, Panea C, Chida AS, et al. Digestion of chromatin in apoptotic cell microparticles prevents autoimmunity. *Cell.* 2016;166(1):88–101. 10.1016/j.cell.2016.05.034 [PubMed: 27293190]
3. Ozcakar ZB, Foster J 2nd, Diaz-Horta O, Kasapcopur O, Fan YS, Yalcinkaya F, Tekin M. DNASE1L3 Mutations in hypocomplementemic urticarial vasculitis syndrome. *Arthritis Rheum.* 2013;65(8):2183–2189. 10.1002/art.38010 [PubMed: 23666765]

4. Ueki M, Kimura-Kataoka K, Takeshita H, Fujihara J, Iida R, Sano R, Nakajima T, Kominato Y, Kawai Y, Yasuda T. Evaluation of all non-synonymous single nucleotide polymorphisms (SNPs) in the genes encoding human deoxyribonuclease I and I-like 3 as a functional SNP potentially implicated in autoimmunity. *FEBS J.* 2014;281(1):376–390. 10.1111/febs.12608 [PubMed: 24206041]
5. Wisniewski JJ, Baer AN, Christensen J, Cupps TR, Flag DN, Jones JV, Katzenstein PL, McFadden ER, McMillen JJ, Pick MA, et al. Hypocomplementemic urticarial vasculitis syndrome. Clinical and serologic findings in 18 patients. *Medicine (Baltimore).* 1995;74(1):24–41. 10.1097/00005792-199501000-00003 [PubMed: 7837968]
6. Mayes MD, Bossini-Castillo L, Gorlova O, Martin JE, Zhou X, Chen WV, Assassi S, Ying J, Tan FK, Arnett FC, et al. Immunochip analysis identifies multiple susceptibility loci for systemic sclerosis. *Am J Hum Genet.* 2014;94(1):47–61. 10.1016/j.ajhg.2013.12.002 [PubMed: 24387989]
7. Almlof JC, Nystedt S, Leonard D, Eloranta ML, Grosso G, Sjowall C, Bengtsson AA, Jonsen A, Gunnarsson I, Svenungsson E, et al. Whole-genome sequencing identifies complex contributions to genetic risk by variants in genes causing monogenic systemic lupus erythematosus. *Hum Genet.* 2019;138(2):141–150. 10.1007/s00439-018-01966-7 [PubMed: 30707351]
8. Hartl J, Serpas L, Wang Y, Rashidfarrokhi A, Perez OA, Sally B, Sisirak V, Soni C, Khodadadi-Jamayran A, Tsigos A, et al. Autoantibody-mediated impairment of DNASE1L3 activity in sporadic systemic lupus erythematosus. *J Exp Med.* 2021;218(5):e20201138. 10.1084/jem.20201138 [PubMed: 33783474]
9. Gomez-Banuelos E, Yu Y, Li J, Cashman KS, Paz M, Trejo-Zambrano MI, Bugrovsky R, Wang Y, Chida AS, Sherman-Baust CA, et al. Affinity maturation generates pathogenic antibodies with dual reactivity to DNase1L3 and dsDNA in systemic lupus erythematosus. *Nat Commun.* 2023;14(1):1388. 10.1038/s41467-023-37083-x [PubMed: 36941260]
10. Weisenburger T, von Neubeck B, Schneider A, Ebert N, Schreyer D, Acs A, Winkler TH. Epistatic interactions between mutations of deoxyribonuclease 1-like 3 and the inhibitory fc gamma receptor IIB result in very early and massive autoantibodies against double-stranded DNA. *Front Immunol.* 2018;9:1551. 10.3389/fimmu.2018.01551 [PubMed: 30026744]
11. Inokuchi S, Mitoma H, Kawano S, Nakano S, Ayano M, Kimoto Y, Akahoshi M, Arinobu Y, Tsukamoto H, Akashi K, et al. Homeostatic milieu induces production of deoxyribonuclease 1-like 3 from myeloid cells. *J Immunol.* 2020;204(8):2088–2097. 10.4049/jimmunol.1901304 [PubMed: 32188756]
12. Engavale M, McCord J, Mapp B, Nzimulinda N, Bengtson E, Sutton RB, Keyel PA. Dnase1 family in autoimmunity. *Encyclopedia.* 2021;1(3):527–541. 10.3390/encyclopedia1030044
13. Napirei M, Karsunky H, Zevnik B, Stephan H, Mannherz HG, Moroy T. Features of systemic lupus erythematosus in Dnase1-deficient mice. *Nat Genet.* 2000;25(2):177–181. 10.1038/76032 [PubMed: 10835632]
14. Lacey KA, Serpas L, Makita S, Wang Y, Rashidfarrokhi A, Soni C, Gonzalez S, Moreira A, Torres VJ, Reizis B. Secreted mammalian DNases protect against systemic bacterial infection by digesting biofilms. *J Exp Med.* 2023;220(6):e20221086. 10.1084/jem.20221086 [PubMed: 36928522]
15. McCord JJ, Engavale M, Masoumzadeh E, Villarreal J, Mapp B, Latham MP, Keyel PA, Sutton RB. Structural features of Dnase1L3 responsible for serum antigen clearance. *Commun Biol.* 2022;5(1):825. 10.1038/s42003-022-03755-5 [PubMed: 35974043]
16. Wilber A, Lu M, Schneider MC. Deoxyribonuclease I-like III is an inducible macrophage barrier to liposomal transfection. *Mol Ther.* 2002;6(1):35–42. 10.1006/mthe.2002.0625 [PubMed: 12095301]
17. Wilber A, O'Connor TP, Lu ML, Karimi A, Schneider MC. Dnase1L3 deficiency in lupus-prone MRL and NZB/W F1 mice. *Clin Exp Immunol.* 2003;134(1):46–52. 10.1046/j.1365-2249.2003.02267.x [PubMed: 12974753]
18. Soni C, Reizis B. Self-DNA at the epicenter of SLE: immunogenic forms, regulation, and effects. *Front Immunol.* 2019;10:1601. 10.3389/fimmu.2019.01601 [PubMed: 31354738]
19. Musapa M, Kumwenda T, Mkulama M, Chishimba S, Norris DE, Thuma PE, Mharakurwa S. A simple chelex protocol for DNA extraction from anopheles spp. *J Vis Exp.* 2013;71:3281. 10.3791/3281

20. Zangala T. Isolation of genomic DNA from mouse tails. *J Vis Exp*. 2007;6:246. 10.3791/246
21. Regna NL, Chafin CB, Hammond SE, Puthiyaveetil AG, Caudell DL, Reilly CM. Class I and II histone deacetylase inhibition by ITF2357 reduces SLE pathogenesis in vivo. *Clin Immunol*. 2014;151(1):29–42. 10.1016/j.clim.2014.01.002 [PubMed: 24503172]
22. Shi G, Abbott KN, Wu W, Salter RD, Keyel PA. Dnase1L3 regulates inflammasome-dependent cytokine secretion. *Front Immunol*. 2017;8:522. 10.3389/fimmu.2017.00522 [PubMed: 28533778]
23. Sekine H, Reilly CM, Molano ID, Garnier G, Circolo A, Ruiz P, Holers VM, Boackle SA, Gilkeson GS. Complement component C3 is not required for full expression of immune complex glomerulonephritis in MRL/lpr mice. *J Immunol*. 2001;166(10):6444–6451. 10.4049/jimmunol.166.10.6444 [PubMed: 11342671]
24. Ray S, Roth R, Keyel PA. Membrane repair triggered by cholesterol-dependent cytolysins is activated by mixed lineage kinases and MEK. *Science Adv*. 2022;8(11):eabl6367. 10.1126/sciadv.abl6367
25. Ray S, Thapa R, Keyel PA. Multiple parameters beyond lipid binding affinity drive cytotoxicity of cholesterol-dependent cytolysins. *Toxins (Basel)*. 2018;11(1):1. 10.3390/toxins11010001 [PubMed: 30577571]
26. Napirei M, Ludwig S, Mezrhah J, Klockl T, Mannherz HG. Murine serum nucleases—contrasting effects of plasmin and heparin on the activities of DNase1 and DNase1-like 3 (DNase1l3). *FEBS J*. 2009;276(4):1059–1073. 10.1111/j.1742-4658.2008.06849.x [PubMed: 19154352]
27. Wang Y, Wang M, Djekidel MN, Chen H, Liu D, Alt FW, Zhang Y. eccDNAs are apoptotic products with high innate immunostimulatory activity. *Nature*. 2021;599(7884):308–314. 10.1038/s41586-021-04009-w [PubMed: 34671165]
28. Serpas L, Chan RWY, Jiang P, Ni M, Sun K, Rashidfarrokhi A, Soni C, Sisirak V, Lee WS, Cheng SH, et al. Dnase1l3 deletion causes aberrations in length and end-motif frequencies in plasma DNA. *Proc Natl Acad Sci U S A*. 2019;116(2):641–649. 10.1073/pnas.1815031116 [PubMed: 30593563]
29. Chan RWY, Serpas L, Ni M, Volpi S, Hiraki LT, Tam LS, Rashidfarrokhi A, Wong PCH, Tam LHP, Wang Y, et al. Plasma DNA profile associated with DNASE1L3 gene mutations: clinical observations, relationships to nuclease substrate preference, and in vivo correction. *Am J Hum Genet*. 2020;107(5):882–894. 10.1016/j.ajhg.2020.09.006 [PubMed: 33022220]
30. Papadimitraki ED, Isenberg DA. Childhood- and adult-onset lupus: an update of similarities and differences. *Expert Rev Clin Immunol*. 2009;5(4):391–403. 10.1586/eci.09.29 [PubMed: 20477036]

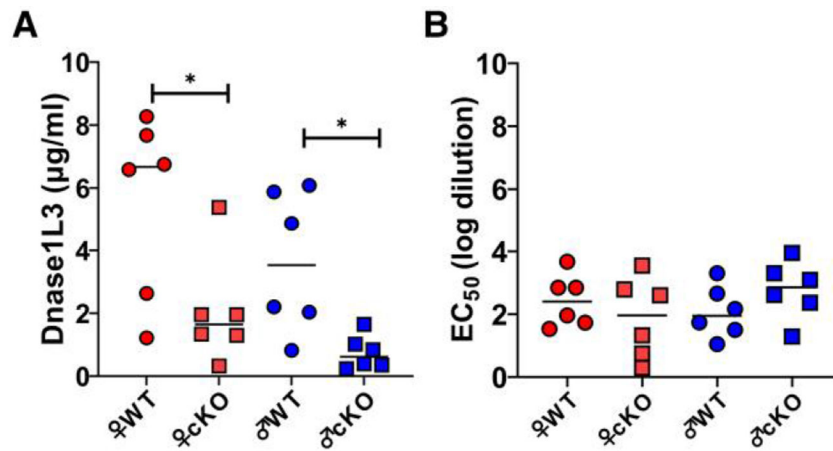


**Fig. 1.**

Dnase1L3 loss from macrophages reduces serum Dnase1L3. (A) Serum Dnase1L3 was measured in 41 to 50 wk old Dnase1L3<sup>fl/fl</sup>×Cre<sup>-/-</sup> (WT) or Dnase1L3<sup>fl/fl</sup>×Cre<sup>+/-</sup> (cKO) mice by ELISA. (B) Serum Dnase1 activity for 41 to 50 wk old WT or cKO mice was measured using 200 ng plasmid DNA for 30 min. The extent of plasmid degradation was quantified and EC<sub>50</sub> calculated as described in the Methods. Data points represent individual mice and median. Six mice per group were used. \**P* < 0.05 by 1-way analysis of variance and Tukey's multiple comparison test.

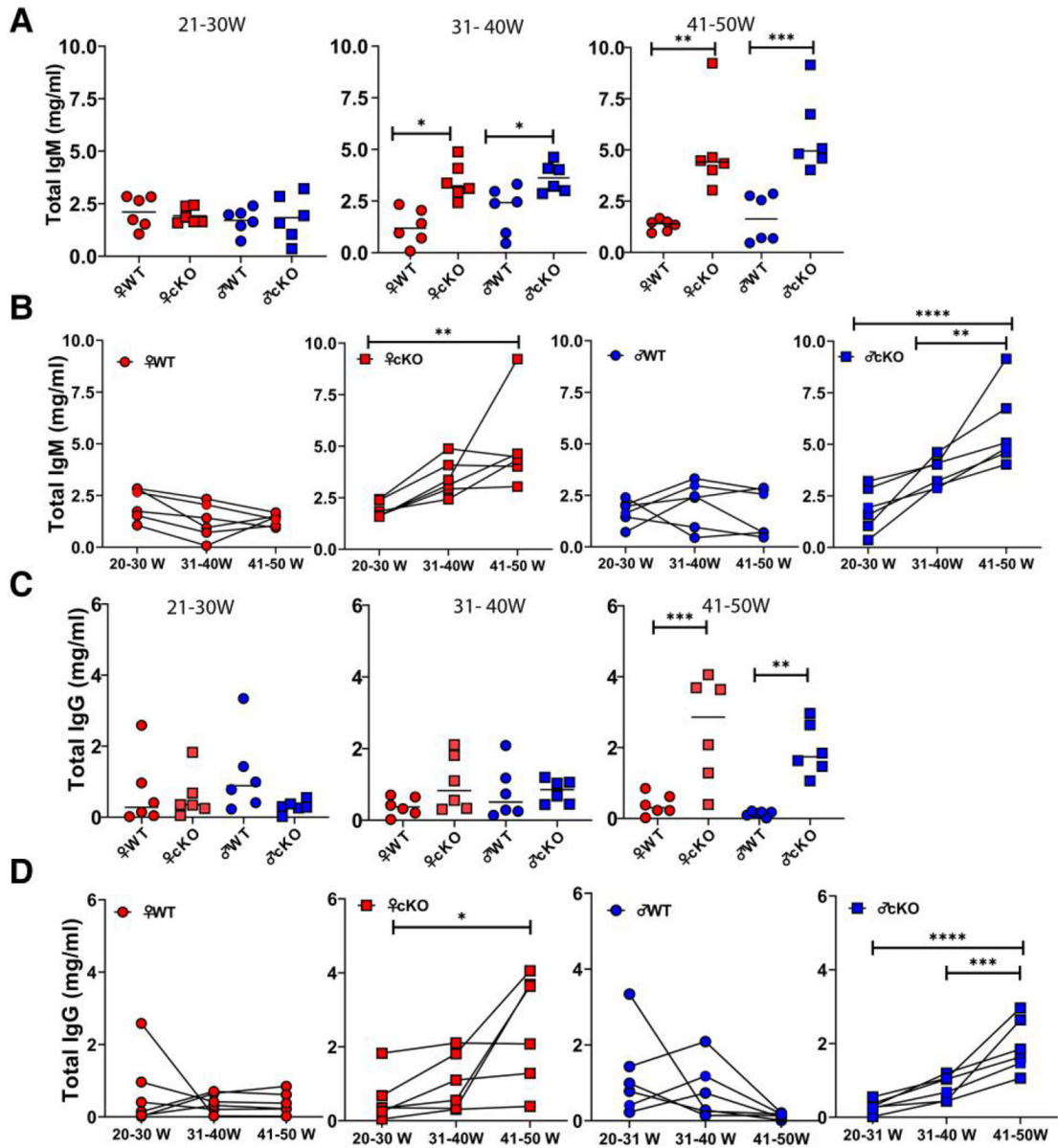


**Fig. 2.** Loss of Dnase1L3 from macrophages causes late elevation of serum IgM and IgG titers. ELISA for IgM or IgG was performed on serially sampled sera from Dnase1L3<sup>fl/fl</sup>×Cre<sup>-/-</sup> (WT) or Dnase1L3<sup>fl/fl</sup>×Cre<sup>+/-</sup> (cKO) mice between 21 to 30 wk, 31 to 40 wk, and 41 to 50 wk. (A) Serum IgM levels at each time point are shown. (B) Progression of serum IgM levels with age for each mouse is shown. (C) Serum IgG levels at each time point are shown. (D) Progression of serum IgG levels with age for each mouse is shown. Graphs show individual mice and median. Six mice per group were used. \*\*\*\**P* < 0.0001, \*\*\**P* < 0.001, \*\**P* < 0.01, and \**P* < 0.05 by 1-way analysis of variance, mixed-effects models, and multiple comparisons using Tukey.



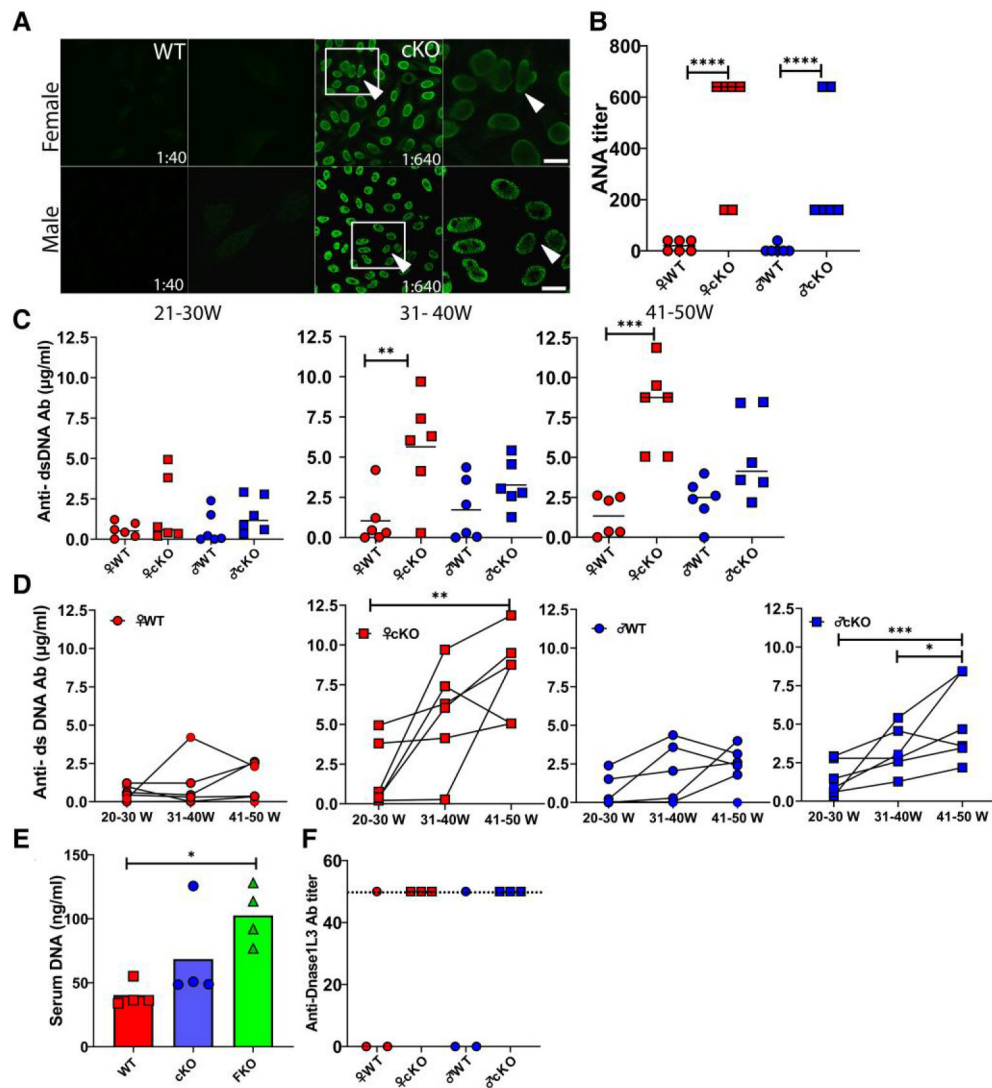


**Fig. 3.** Mice lacking macrophage Dnase1L3 produce anti-nuclear antibodies, anti-dsDNA antibodies, and anti-Dnase1L3 antibodies. Fixed HEp2 cells were incubated with sera from 41- to 50-wk-old mice at 1:40, 1:160, or 1:640 dilutions and stained with anti-mouse IgG (green). (A) Micrographs show a representative field at the indicated dilution. Scale bar = 50 µM (B) Quantitation of ANA titer. (C, D) ELISA for anti-dsDNA was performed on serially sampled sera from *Dnase1L3<sup>fl/fl</sup>×Cre<sup>-/-</sup>* (WT) or *Dnase1L3<sup>fl/fl</sup>×Cre<sup>+/-</sup>* (cKO) mice between 21 to 30 wk, 31 to 40 wk, and 41 to 50 wk. (C) Anti-dsDNA levels at each time point are shown. (D) Progression of anti-dsDNA levels with age for each mouse is shown. (E) Serum DNA was measured in WT, cKO, or *Dnase1L<sup>-/-</sup>* (FKO) mice. (F) Anti-Dnase1L3 antibodies were measured at a 1:50 serum dilution and considered positive if the  $A_{450}$  was  $>0.1$ . The dashed line represents the limit of detection. Data points represent individual mice. Graphs show individual mice and median. (A-D) Six, (E) 4, or (F) 3 mice per group were used. \*\*\*\* $P < 0.0001$ , \*\*\* $P < 0.001$ , \*\* $P < 0.01$ , and \* $P < 0.05$  by 1-way analysis of variance, mixed-effects models, and multiple comparisons using Tukey.

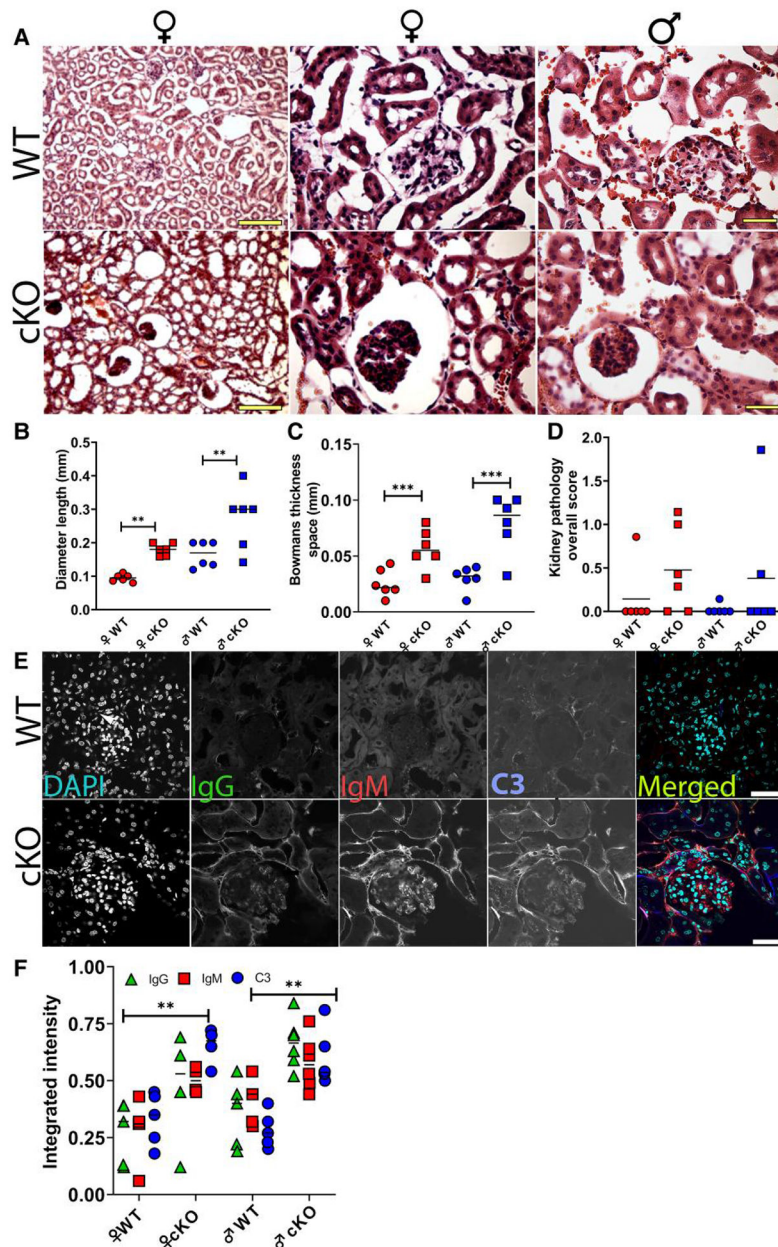


**Fig. 4.** Dnase1L3 loss from macrophages causes mild kidney phenotypes. (A) Kidney sections from 50-wk-old Dnase1L3<sup>fl/fl</sup>×Cre<sup>-/-</sup> (WT) or Dnase1L3<sup>fl/fl</sup>×Cre<sup>+/-</sup> (cKO) mice were stained with hematoxylin and eosin. A representative glomerulus in the inset is shown. (B, C) Glomerular diameter and Bowman's capsule space were quantitated. (D) The degree of kidney pathology was measured for each mouse. (E) Kidney sections from 50-wk-old Dnase1L3<sup>fl/fl</sup>×Cre<sup>-/-</sup> (WT) or Dnase1L3<sup>fl/fl</sup>×Cre<sup>+/-</sup> (cKO) mice were stained with anti-mouse IgG Alexa Fluor 488 (green), DAPI (cyan), anti-mouse IgM Cy3 (red), and anti-C3 Alexa 647 (blue), and imaged by confocal microscopy. (F) Quantitation of the fluorescence intensity for each antibody. (A, E) Representative micrographs from 6 animals per group are shown. (B-D, F) Graphs show 6 individual mice per group plus the median for each

phenotype. Scale bar = 50  $\mu\text{m}$  \*\*\* $P < 0.005$  and \*\* $P < 0.01$  by 1-way analysis of variance and Tukey's multiple comparison test.

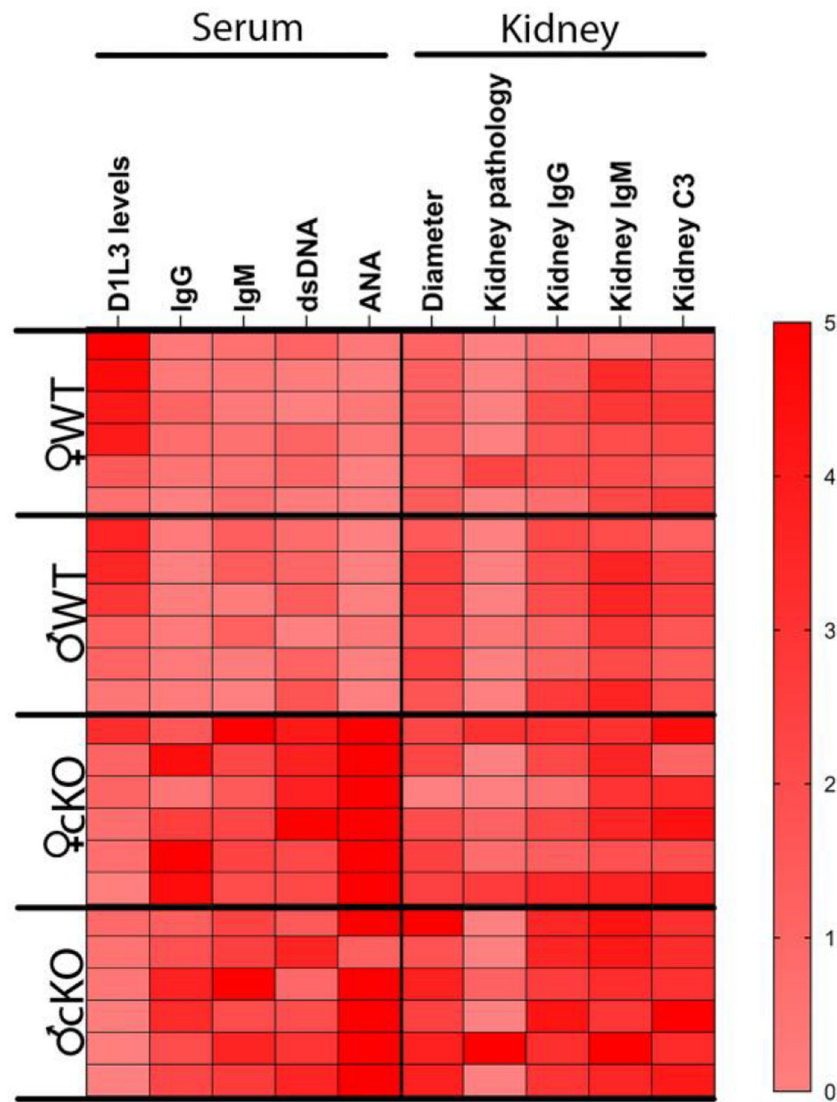


**Fig. 5.** Reduction in Dnase1L3 levels associates with lupus-like phenotypes in mice. Dnase1L3 levels and lupus-like phenotypes were each normalized to a 5-point linear scale, in which 5 represents the phenotype of the most affected mouse and 0 represents the least affected mouse. Each row represents an individual Dnase1L3<sup>fl/fl</sup>×Cre<sup>-/-</sup> (WT) or Dnase1L3<sup>fl/fl</sup>×Cre<sup>+/-</sup> (cKO) mouse.